Shock Response of a Zirconium-based Bulk Metallic Glass

Fuping Yuan, Vikas Prakash and John J. Lewandowski*

Department of Mechanical and Aerospace Engineering

*Department of Materials Science and Engineering

Case Western Reserve University

ABSTRACT

Results are presented on the shock response of a zirconium-based bulk metallic glass (BMG), $Zr_{41.25}Ti_{13.75}Ni_{10}Cu_{12.5}Be_{22.5}$, subjected to planar impact loading. Two series of plate impact experiments are conducted to:

(a) Estimate spall strength of the BMG following different levels of normal shock compression, combined shock compression with shear loading.
(b) Study the dependence of flow stress in shear on ultra-high strain rates (~10^6 /s), high normal stresses (up to 9 GPa) and high hydrostatic pressures (up to 6 GPa).

The first series of experiments show that the spall strength decreases with increasing levels of normal shock-compression. In the combined compression-shear plate-impact spall experiments, with increasing levels of shear strain, the spall strength is observed to decrease initially, increase dramatically, and then decrease again as the shear strain is increased from 2.4% to 3.2%.

The second series of experiments indicate the hydrostatic pressure has a negligible influence on the flow stress in shear up to 6 GPa. The normal-stress has a negligible influence on the flow stress during compression (0.78 - 8.8 GPa), while it has a small influence when the stress state changes from compression to tension. Moreover, the high strain rate experiments show that rate sensitivity of this BMG is negligible up to strain rates of 10^5 /s.

MATERIAL: $Zr_{41.25}Ti_{13.75}Ni_{10}Cu_{12.5}Be_{22.5}$ (LM-1)

- High strength (≈ 2 GPa under uniaxial stress).
- Large elastic strain (≈ 2% under uniaxial stress).
- High hardness, excellent wear and corrosion resistance.
- Increased fracture toughness when compared to other brittle, high compressive strength materials.
- Low critical cooling rate (1-10 K/s vs. 10^6 K/s).
  - Thick plates (e.g., 10 mm) can be produced.
- The shock response of BMGs is of considerable interest for potential applications, such as:
  - Kinetic energy penetrators and composite armor.
  - Sports, medical implants and coatings.

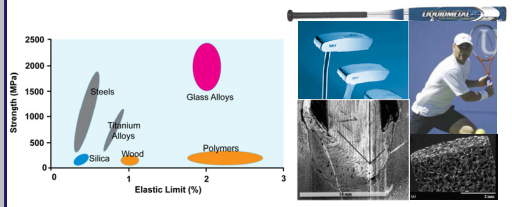

(a) (b)

Figure 1: (a) Typical strengths and elastic limits for various materials. (b) Applications of BMG.

MATERIAL PREPARATION

- Spall strength under normal shock compression, and combined compression with shear loading.
  - Plate dimensions: 90 mm x 63 mm x 5 mm.
  - Circular disks were EDM machined: diameter 25.4 mm, thickness ~4.5 mm.
  - EDM disks were lapped and polished to a surface finish of 5 micrometers.
- Flow stress in shear under ultra-high strain rates, high normal stresses and high hydrostatic pressures.
  - Thin square plates: 38 mm x 38 mm x 0.7 mm.
  - Lapped and polished to a surface finish of 5 micrometers and thickness of ~ 0.6 mm
- DSC and XRD reveal that LM-1 is fully amorphous.
- EDM and polished disks remained fully amorphous.

EXPERIMENTAL TECHNIQUES

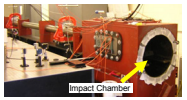

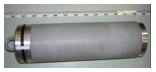

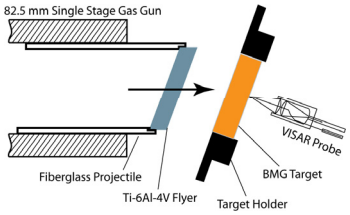

Figure 2: Schematic of the plate impact pressure with shear spall experiment.

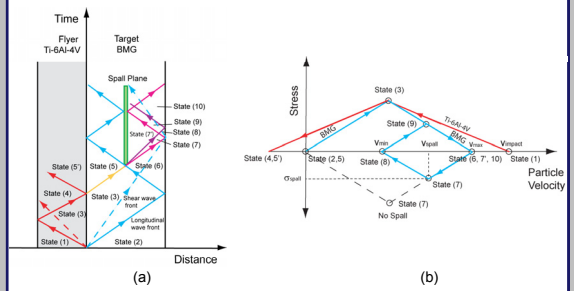

(a) (b)

Figure 3: (a) Time-distance diagram for spall experiments. (b) Stress-velocity diagram for spall experiments.

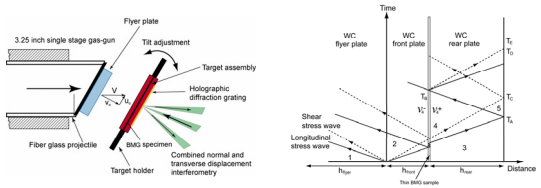

(a) (b)

Figure 4: (a) Schematic of pressure with shear sandwich experiments. (b) Time-distance diagram for sandwich experiments.

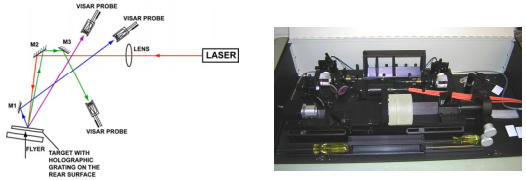

(a) (b)

Figure 5: (a) Schematic of the combined normal and transverse velocity interferometer. (b) VISAR.

NORMAL SHOCK COMPRESSION SPALL RESULTS

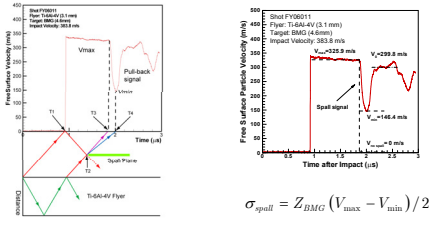

$$\sigma_{spall} = Z_{BMG}\left(V_{max} - V_{min}\right)/2$$

(a) (b)

Figure 6: (a) Time-distance diagram paired with the measured free-surface particle velocity profile for experiment FY06011 to illustrate the "pull-back spall signal". (b) Free surface particle velocity data for experiment Shot FY06011. Spall strength can be calculated from the "pull-back spall signal" using the equation shown.

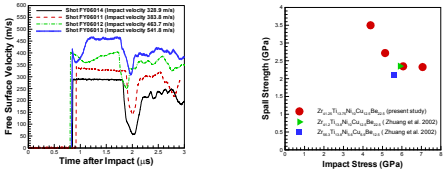

(a) (b)

Figure 7: (a) Free surface particle velocity versus time profiles for the four normal plate-impact spall experiments. (b) Spall strength as a function of impact Stress for three different Zr-based BMGs.

PRESSURE WITH SHEAR SPALL RESULTS

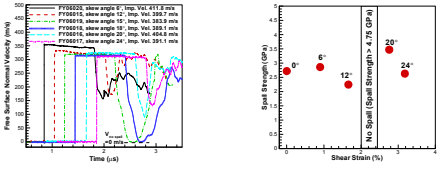

(a) (b)

Figure 8: (a) Free surface particle velocity versus time profiles for the six pressure-shear plate-impact spall experiments. (b) Spall strength as a function of shear strain.

SEM PICTURES OF THE SPALL PLANES

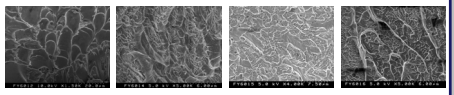

Figure 9: (a) Shot FY06012 Normal impact (Normal stress below HEL) (b) Shot FY06014 Normal impact (Normal stress above HEL) (c) Shot FY06015 Skew angle 12º (Normal stress below HEL) (b) Shot FY06016 Skew angle 20º (Normal stress below HEL)

RESULTS OF HIGH STRAIN RATE COMBINED COMPRESSION WITH SHEAR EXPERIMENTS

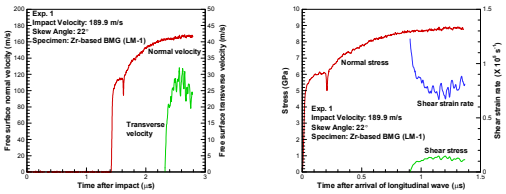

(a) (b)

Figure 10: (a) Longitudinal and transverse free surface velocities for Exp. 1. (b) History of normal stress, the shear stress and the shear strain rate in the specimen for Exp. 1.

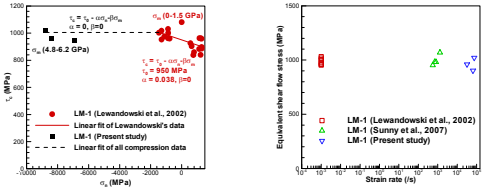

(a) (b)

Figure 11: (a) Dynamic shear stress versus shear strain for Exp. 1. (b) Equivalent shear flow stress versus strain rate.

SUMMARY

- The spall strength of this BMG under normal shock compression was found to decrease with increasing normal stress below the HEL (6.15 GPa), and then remains nearly constant above the HEL.
- The spall strength under combined compression with shear loading was found to
  - Initially slightly decrease with increasing levels of shear strain, and
  - Then increase dramatically (> 3.5 GPa), and no spall was observed at ~ 2% shear strain.
  - Followed by a decrease in spall strength as the shear strain was increased from 2.40% to 3.18%.
- The trend in the effects of normal stress and shear strain on the spall strength of the BMG can perhaps be explained by the competing roles of localized plasticity and shock/shear-induced damage taking into consideration their relative dominance below and above a critical normal stress/shear strain.
- In the high strain rate combined compression with shear experiments, a weak dependence of flow stress in shear on ultra-high strain rates (~10^5 /s), high normal stresses (up to 9 GPa) and high hydrostatic pressures (up to 6 GPa) was observed for this BMG.

ACKNOWLEDGMENTS

The authors would like to acknowledge Case Prime Fellowship and the Office of Naval Research (ONR-N00014-03-1-0205) for providing the financial support for conducting the present research. The authors would also like to acknowledge the Major Research Instrumentation Award CMS-0079458 and CMMI 0521364 by the NSF for the acquisition of the Multi-beam VALYN VISAR and the scanning electron microscope (FEI FE NanoSEM600), respectively.

REFERENCES

1. Lewandowski, J. J., and Lowhaphandu, P., 2002. Effects of hydrostatic pressure on the flow and fracture of a bulk amorphous metal. Philosophical magazine. vol. A82 (17/18), pp. 3427-3441.
2. Martin M., Sekine, T., Kobayashi T., Kecskes, L. and Thadhani, N. N., 2007. High-pressure equation of the state of a Zirconium-based bulk metallic glass. Metallurgical and Materials Transactions A, DOI: 10.1007/s11661-007-9263-x.
3. Zhuang, S. M., Lu, J., and Ravichandran, G., 2002. Shock wave response of a zirconium-based bulk metallic glass and its composite. Applied Physics Letters 80, 4522-4524.
4. Yuan, F., Prakash, V., and Lewandowski, J. J., 2007. Spall strength and Hugoniot elastic limit of a Zirconium-based bulk metallic glass under planar shock compression. Journal of Materials Research. vol. 22 (2), pp. 402-411.
5. Yuan, F., Prakash, V. and Lewandowski J.J. , 2007. Spall Strength of a Zirconium-based Bulk Metallic Glass under Shock Compression and Shear Loading. Submitted to Journal of the Mechanics and Physics of Solids.
6. Yuan, F., Prakash, V. and Lewandowski J.J. , 2007. Pressure Effects on the Flow Stress of a Zirconium-based Bulk Metallic Glass, Submitted to Journal of the Mechanics and Physics of Solids.